creative commons
COMMONS DEED

저작자표시-비영리-변경금지 2.0 대한민국

이용자는 아래의 조건을 따르는 경우에 한하여 자유롭게

- 이 저작물을 복제, 배포, 전송, 전시, 공연 및 방송할 수 있습니다.

다음과 같은 조건을 따라야 합니다:

저작자표시. 귀하는 원저작자를 표시하여야 합니다.

비영리. 귀하는 이 저작물을 영리 목적으로 이용할 수 없습니다.

변경금지. 귀하는 이 저작물을 개작, 변형 또는 가공할 수 없습니다.

- 귀하는, 이 저작물의 재이용이나 배포의 경우, 이 저작물에 적용된 이용허락조건을 명확하게 나타내어야 합니다.
- 저작권자로부터 별도의 허가를 받으면 이러한 조건들은 적용되지 않습니다.

저작권법에 따른 이용자의 권리는 위의 내용에 의하여 영향을 받지 않습니다.

이것은 이용허락규약(Legal Code)을 이해하기 쉽게 요약한 것입니다.

Disclaimer

dCollection

Project Report of Master of Engineering

Deep Learning Analysis of Thermographic Images for Contactless PCBA Defect Detection

비접촉식 PCBA 불량 검출을 위한 열화상 이미지의 딥러닝 분석

February 2021

Graduate School of Engineering Practice
Seoul National University
Department of Engineering Practice

Siyun Yoo

Deep Learning Analysis of Thermographic Images for Contactless PCBA Defect Detection

비접촉식 PCBA 불량 검출을 위한 열화상 이미지의 딥러닝 분석

Professor Seong-Woo Kim

Submitting a Master's Project Report

February 2021

Graduate School of Engineering Practice

Seoul National University

Department of Engineering Practice

Siyun Yoo

Confirming the master's Project Report written by

Siyun Yoo

February 2021

Chair	Wooyoung Kwak	(Seal)
Examiner	Seong-Woo Kim	(Seal)
Examiner	Changwoo Park	(Seal)

Abstract

For mass production of electronic products, in-circuit-test (ICT) method is applied and a printed circuit board assembly (PCBA) quality test is performed. The in-circuit test method has the advantage of being able to measure resistance values and capacitance. However, since the in-circuit test method requires the use of a fixture, it is expensive in terms of price and has a disadvantage that it must be replaced frequently. The needle used for the fixture may cause PCBA defects.

In this paper, we propose a non-contact test method that can detect PCBA defects without applying the fixture and in-circuit test methods. This is a non-contact defect detection method through comparison of thermal images and deep learning analysis. Vision inspection methods cannot be applied to parts inspection, e.g. chip resistance, chip capacitors, that does not have external visible characteristics. We review the existing non-contact test method and compare it with the proposed thermal image analysis method. Thermal images are reviewed by applying SSIM as a rule-based object detection methods, and CNN, RCNN, AutoEncoder as deep learning analysis methods.

Keywords : contactless inspection, deep learning, defect detection, thermographic image

Student Number : 2019-27335

Contents

I. Introduction **1**

1.1 Field problems 1

1.2 Approach and limitation of existing research 2

1.2.1 Vision measurement method 3

1.2.2 EM wave measurement method 4

1.2.3 Infrared thermal measurement 6

1.2.4 Hyperspectral image Test 9

1.2.5 Ultrasonic Test 9

1.3 Proposal 10

II. Related Works **13**

2.1 Thermal image measurement 13

2.2 Thermal image analysis 15

2.3 Rule-based object detection 18

2.3.1 SIFT 18

2.3.2 PSNR and SSIM 20

2.4 Deep learning analysis 22

2.4.1 CNN 22

2.4.2 AutoEncoder 25

2.4.3 One-shot learning 27

III. Problem definition and proposed methods **29**

3.1 Problem definition 30
3.2 Proposed methods 31
3.2.1 Rule based method 31
3.2.2 Deep learning based method 32

IV. Experiment and evaluation 36
4.1 Dataset definition and construction 36
4.2 Progress and results 40
4.2.1 SSIM 40
4.2.2 CNN 42
4.2.3 RCNN 46
4.2.4 AutoEncoder 47

V. Conclusion and evaluation 51
5.1 Conclusion 51
5.2 Lessons and Learned 52
5.3 Limitations of research and future research 54

Bibliography 56

Abstract 61

List of Figures

Figure 1. Test point and Fixture for ICT method. 1
Figure 2. PCB Image comparison for defect detection. 3
Figure 3. Near field electromagnetic test. 4
Figure 4. Electromagnetic field test with test bed. 5
Figure 5. Sample test result. 6
Figure 6. Power dissipation of capacitors. 7
Figure 7. Defect detection by changing C4 capacitance. 8
Figure 8. Hyperspectral test of resistor. 10
Figure 9. Emissivity of the object. 16
Figure 10.SIFT 18
Figure 11.Max pooling 23
Figure 12.Skip connection. 24
Figure 13.AutoEncoder. 26
Figure 14.Siamese Network 27
Figure 15.Vision Test vs IR Test 29
Figure 16.Frequency resistor change : 40kohm to 20kohm. 34
Figure 17.Setting Frequency and current consumption change. . . . 35
Figure 18.Test environment for thermal image acquisition. 37
Figure 19.Thermal Image by thermal imaging camera. 37
Figure 20.Image extraction by time. 38
Figure 21.No.1 - Free angle, Fixed angle. 39

Figure 22.No.2 - Transient 10s, 20s, 30s, 40s. 39
Figure 23.No.3 - Rotation ±5°, ±10°. 40
Figure 24.Image comparison with SSIM. 41
Figure 25.Disadvantages of SSIM. 41
Figure 26.CNN Test Dataset. 43
Figure 27.CNN Model. 43
Figure 28.CNN result 44
Figure 29.Accuracy in power-on time. 45
Figure 30.Accuracy on camera angle. 46
Figure 31.Region proposal with 50 area. 47
Figure 32.Test Result with RCNN. 48
Figure 33.AutoEncoder Test: Resized image input. 49
Figure 34.AutoEncoder Test: Original High-Quality image input. . . 49
Figure 35.AutoEncoder Test: Fixed image input. 50
Figure 36.AutoEncoder Test: Defect detection. 50
Figure 37.Project all flow 55

List of Tables

Table 1. ICT Pros and Cons. 2

Table 2. Comparison of defect detection and productivity. 11

Table 3. Qualitative evaluation. 12

Table 4. Advantages of thermal imaging. 14

Table 5. CNN Model 23

Table 6. Confusion Matrix. 31

Table 7. Different method for thermal test. 34

Table 8. PCBA Thermal image Dataset. 39

Table 9. Deep learning analysis method. 52

Chapter 1

Introduction

1.1 Field problems

The electronics industry basically uses a printed circuit board (PCB), and with the development of surface mount technology (SMT), many parts are automatically arranged and soldered. Mass-produced PCB Assembly (PCBA) through an automated system is subjected to various quality inspections for required performance inspection. PCBA quality inspection uses In-Circuit-Test (ICT) method with Test point and fixture in Figure 1.

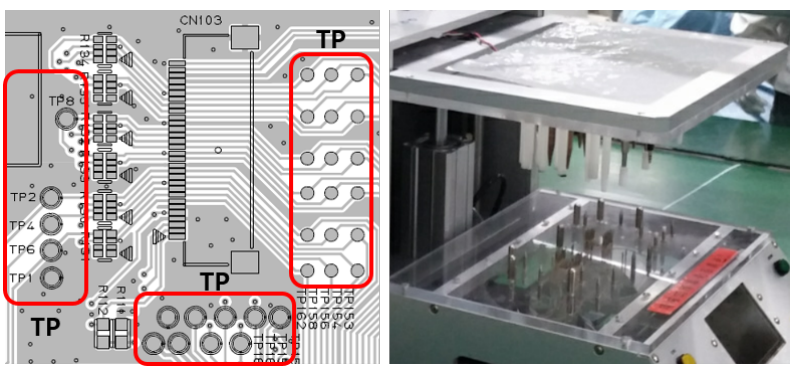

Figure 1: Test point and Fixture for ICT method.

In Table 1, The ICT method is an easy method in the mass production system, and it is a method that can accurately identify defective parts, but it causes cost problems such as expensive fixture manufacturing costs and periodic fixture replacement costs. In addition, the use of the bed-of-nail type

fixing table gives an electric shock such as ESD to the PCBA because many needles directly contact the PCBA, and physically causes component damage (backdriving). In terms of design, in order to cope with ICT, it is difficult to cope with miniaturized electronic product design because TP (Test Point) must be added for each pattern when designing a PCB. There is a need for a way to supplement the shortcomings of the contact-type ICT method, secure productivity, and increase accuracy.

Table 1: ICT Pros and Cons.

Pros
- Easy to detect defects : Continuous defect detection - With simple test program - Clear judgment results
Cons
- Expensive fixtures - Periodic replacement of fixtures - ESD Shock and Back Driving - Impossible test access by integration

1.2 Approach and limitation of existing research

Several non-contact test methods were considered to replace the contact ICT method. The approaches of the existing research can be divided into a vision measurement method that measures external characteristics, an electromagnetic wave measurement method using electromagnetic waves and heat generated during operation, and a thermal measurement method.

1.2.1 Vision measurement method

The vision measurement method includes a traditional visual inspection method and refers to a computer vision inspection method using a camera. As a method of conducting a defect inspection through the comparison of a genuine product and a defective product, a deep learning analysis method has recently been introduced to perform a fast and accurate inspection [1].

Defects can be found by external features of the PCB, and defects can be found through image comparison as shown in Figure 2 [2] [3]. Regarding the detection of defects in the PCBA's placement, three methods were suggested. Background subtraction, template matching, and wavelet transform. With these methods, it was possible to successfully identify missing or misaligned parts. The wavelet transform has the advantage of taking less execution time compared to the other two methods.

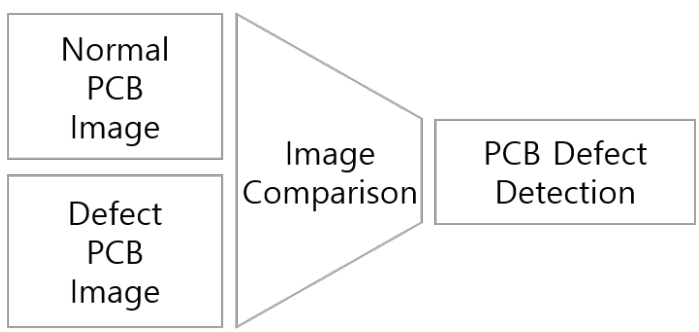

Figure 2: PCB Image comparison for defect detection.

However, in order to apply the vision measurement method, the object must have externally different characteristics. Among the components on the PCBA, chip resistors and chip capacitors look the same outwardly, but re-

sistance values and capacitance values are different. In addition, in case of internal damage to the component, Defect cannot be detected.

1.2.2 EM wave measurement method

In order to find defects in parts that do not show different characteristics externally, we approach defect detection by measuring electromagnetic waves according to the characteristics of parts. In the ICT method, resistance measurement is performed through V-I measurement, and capacitor measurement is performed through a full-band frequency scan. The electromagnetic wave measurement method measures the electromagnetic waves generated by each component in the process of applying power to the PCBA and consuming current. NEB Alaoui changed the output capacitance values of the DCDC power supply and measured the change of the generated electromagnetic waves [4].

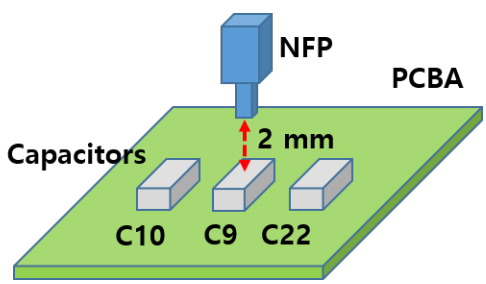

Figure 3: Near field electromagnetic test.

A Near Field electromagnetic Probe (NFP) was placed 2 mm above the capacitor as shown in Figure 3. Capacitance value of capacitors was changed, and the Fast Fourier Transform (FFT) value was measured. The measured value of the reference capacitor and the measured value of the changed ca-

pacitor are different. Through this, the possibility of non-contact diagnosis of defective components using electromagnetic signals was presented.

However, the near-electromagnetic field measurement method is a measurement method applied only to a DCDC power supply and a specific part, and is difficult to apply to the entire system. Appropriate amplification and signal conditioning should be considered to increase measurement sensitivity and set detection limits.

Furthermore, for measuring a wide range of electromagnetic waves, a method using a test bed and UUT (Unit Under Test) was also presented [5]. The electromagnetic wave generated from the signal line is read through the test bed, and the voltage ratio according to the applied frequency is measured through the network analyzer as shown in Figure 4.

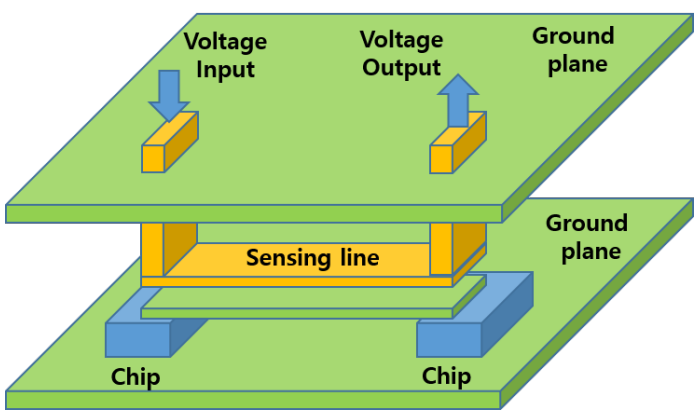

Figure 4: Electromagnetic field test with test bed.

By measuring the electromagnetic wave of the signal line of the SD card of the UUT, it can be confirmed that there is a significant margin difference between the original product PCBA voltage ratio and the defective product

PCBA voltage ratio around the resonance frequency in Figure 5.

However, the non-contact electromagnetic wave measurement method using a test bed is disadvantageous to be applied to a manufacturing line that requires low cost and productivity. As the cost of the existing ICT contact type fixed bed is consumed, the test bed method incurs additional costs. Test bed production has a disadvantage that it cannot be reused because it must be manufactured according to the production model.

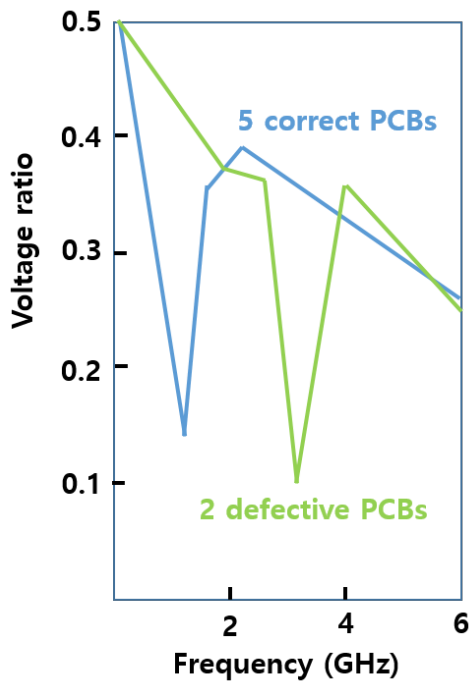

Figure 5: Sample test result.

1.2.3 Infrared thermal measurement

In the case of passive elements such as capacitors that do not have external characteristics, defects are measured using heat generated in the operating

state [6] [7] [8]. Measured heat of the passive elements compare normal heat data to check whether a component is defective. In the DCDC power supply unit, a ripple current flows through the output capacitor due to a switching operation, energy is consumed due to the residual current flowing through the capacitor, and energy is dissipated as heat in Figure 6.

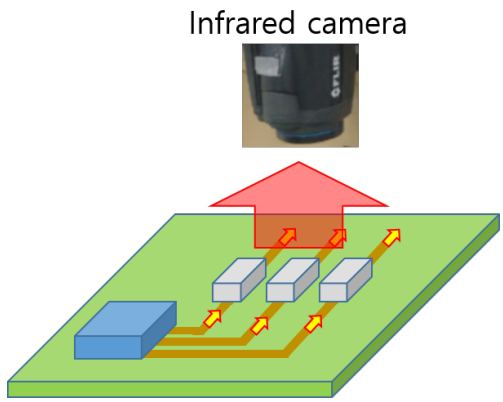

Figure 6: Power dissipation of capacitors.

Power is dissipated (Pd) as residual current (Icrms) flows through the Equivalent Series Resistance (ESR) inside the capacitor as Equation (1.1).

$$Pd = (ESR)(Icrms)^2. \tag{1.1}$$

If the change in the temperature of the capacitor with respect to time is expressed as an integral formula, it can be seen that the temperature of the capacitor (Tc) is proportional (A) to the energy consumption (Pd) over time (t) as Equation (1.2).

$$Tc = A(Pd, t). \tag{1.2}$$

Among the output capacitors, one capacitor is selected (C4), the capacitance is changed, and each temperature is measured according to the time change. As the time changes, the energy consumed increases and the temperature gradually rises as shown in the graph. Each measured value was compared with other capacitors around it, and was calculated as a mean square error (MSE) value and expressed as a graph. As shown in Figure 7, faulty parts can be found because the MSE value is different from normal parts.

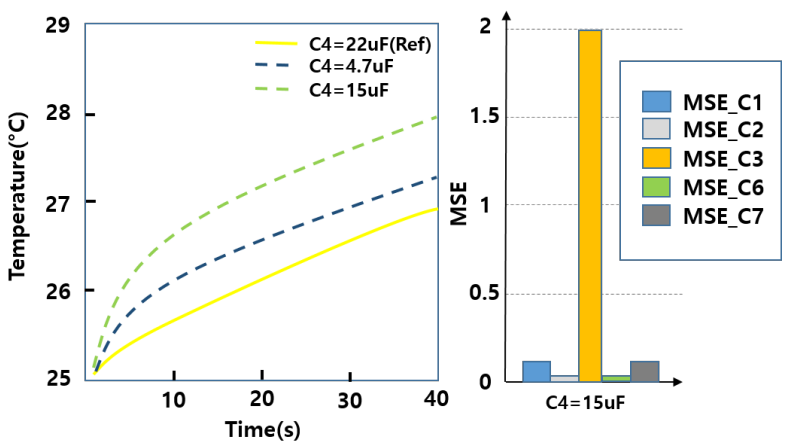

Figure 7: Defect detection by changing C4 capacitance.

In order to find defective capacitors in a limited area of PCBA, an infrared thermal measurement method was proposed as a non-contact test method. However, the thermal measurement method consumes a lot of time for testing because it has to wait for the PCBA to be thermally saturated. In addition, it

has the disadvantage that the temperature change is not constant due to the surrounding environment. Since the proposed method is a result of the PCBA limited area, additional verification is required in the entire PCBA area.

1.2.4 Hyperspectral image Test

The hyperspectral camera subdivides hundreds of wavelength information in the wavelength band in the visible range 400-700 nm. The object to be measured is an image of the electromagnetic spectrum, and objects and materials are identified and detected. It is being used in new businesses such as electronic devices, robotics, biotechnology, and healthcare. Hyperspectral imaging devices in the medical field are widely used to diagnose diseases, cancer, and skin. In the field of environmental monitoring, hyperspectral images are used for forest management, precision agriculture, and pollution control [9].

The resistance characteristics were checked using a hyperspectral camera, but the internal material of the chip resistance could not be confirmed. In this case, it was similar with vision test such as Figure 8.

1.2.5 Ultrasonic Test

The representative method of non-destructive testing is ultrasound. A phased array ultrasonic flaw detection device of a probe in which a plurality of vibrators are arranged in phase difference is widely used not only in the medical field but also in the industrial field. It is mainly applied to the field to accurately measure the speed of ultrasonic waves and inspection of moving

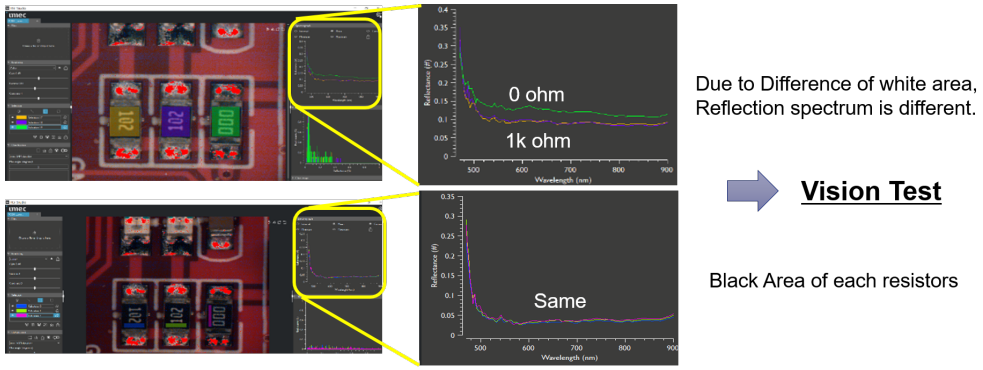

Figure 8: Hyperspectral test of resistor.

objects using electronic ultrasonic waves [10] [11].

The inspection results have to rely on the inspector's inspection report, and it is difficult to identify the type of defect. There is a disadvantage in that it is easy to be affected by the metal structure. Also, if the surface is not smooth, a clean reflected signal cannot be obtained.

1.3 Proposal

There is a need to solve various problems such as increase in production cost caused by application of existing ICT technology, PCBA destruction due to contact test, and difficulty in PCB design due to TP addition. For this, various non-contact test methods were reviewed. The defect detection power and productivity of the vision test, electromagnetic wave test, thermal measurement test, ultrasonic test, and hyperspectral camera test methods were compared in Table 2.

Based on the productivity and performance evaluation, the test takes a lot of time, but we propose a thermal imaging camera test method that can detect

Table 2: Comparison of defect detection and productivity.

Test	Abnormal Value	Defect part	Cost	Time
Vision Test	X	O	L	L
Hyperspectral image	X	O	M	L
Thermographic image	O	O	L	H
Ultrasonic test	O	O	M	H
EM wave test	O	O	H	M

all defects and is advantageous in terms of cost. We propose a contactless test method that analyzes the thermal image data of the entire PCBA through deep learning and verifies its possibility.

Deep learning analysis is used on various industrial area. M.Sharp present the current status and gap of machine learning applications of manufacturing industry [12]. And, J. Wang show the methods and applications of deep learning for smart manufacturing. CNN model is used for surface integration inspection. AE and RNNs are used for Machinery fault diagnosis and predictive analytics and defect prognosis [13]. And, For detecting fault of surface, CNN is used. 12 sample materials are used for training with 2 convolution layers and 2 pooling layers. 260 times Higher performance than manpower inspection and lower human hiring cost can be performed with machine learning in smart manufacturing as shown in Table 3 [14].

The structure of this paper is as follows.

In Chapter 2, we study thermal image measurement and image processing methods, and study methods that can analyze the measured thermal image through rule-based object detection methods and various deep learning methods. In Chapter 3, our proposal is clearly described. In Chapter 4 presents the

Table 3: Qualitative evaluation.

	CNN methods	Manpower inspection
Accuracy	98%	98.5%
Speed(sample/min)	5285	20
Duration	All day	Limited time
Defect type	Various	Specific defect

experimental results applying several deep learning analysis techniques. And, the dataset used in this study is explained. Finally, In Chapter 5 concludes this work by evaluating the research content described in this paper and describing it along with future research direction.

In order to respond to the problems that occurred while applying the existing ICT method and improve productivity, this research method is proposed. By measuring thermal images of products that are actually being mass-produced, a thermal dataset is constructed, and the possibility of detecting PCBA defects through thermal images is proposed. It helps to detect defects by quickly discovering whether there is a defect, not a specific point defect.

Chapter 2

Related Works

2.1 Thermal image measurement

A typical non-contact type temperature measuring device is a thermal imaging camera. It detects infrared energy radiated, transmitted, and reflected from an object above the absolute temperature of 0 degrees. The sensed energy is converted into a temperature reading or a temperature record. This temperature record is output as a thermal image of an object that is a heat source of infrared energy. Conventional infrared thermometers display only a single temperature measured in a limited single area, while thermal imaging cameras display an overall thermal image of up to 19,600 areas.

The thermal imaging camera uses an infrared region after the visible light region (0.35 μm-0.75 μm) of the electromagnetic wave region. The infrared region is composed of near-infrared rays (0.75 μm-1.5 μm), mid-infrared rays (1.5 μm-20 μm), and far infrared rays (20 μm-1000 μm). Objects radiate light rays in the infrared region. Even very cold objects, such as ice, radiate infrared rays.

Thermal image measurement has many advantages as shown in Table 4. Non-contact/remote monitoring is possible, and real-time measurement is possible even at night without light. It provides two-dimensional (2D) analy-

sis information. It is used in various fields such as construction and electricity/electronics, and is used as a method for discovering current or potential problems.

Table 4: Advantages of thermal imaging.

Contactless/remote monitoring
- Non-exposure of the operator to risk - Non-interfere to management targets - Facility management in operation
Real-time measurement
- Rapid observation of suspended targets - Immediate capture of rapidly changing - Real-time changing thermal pattern capture
2D analysis information
- Comparison between targets - Visual expression of thermal patterns

Thermal imaging cameras measure the radiant heat of an object. The amount of energy entering an object is equal to the sum of the amount of reflection, transmission, and absorption according to the law of conservation of energy. However, the radiant energy emitted by an object differs depending on the composition of the object. So, in theory, a black body was defined as an object that absorbs or reflects all incident radiation. The characteristics of a blackbody can be confirmed by Plank's law, Wien's displacement law, and Stefan-Boltzmann's law.

In 1900, Max Planck expressed the energy radiation through a blackbody. Planck's law is a law in which the energy emitted according to wavelength and temperature changes, and it can be seen that the solar radiation energy

measured in the upper atmosphere and the energy result according to Planck's law are almost identical.

The energy emitted varies with wavelength and temperature in Wien's law. It can be seen that the higher the temperature, the shorter the wavelength at which the maximum energy appears.

$$P = e\sigma AT^4. \tag{2.1}$$

Where e is the emissivity of the grey body, σ is the Stefan–Boltzmann constant (σ = 5.67036710^{-8} W/(m^2K^4)), A is surface area and T is black body's thermodynamic temperature.

Equation (2.1) is Stefan-Boltzmann law which multiplies the Plank's law formula by π to convert radiance into irradiance. It can be seen that the total radiant energy emitted by a blackbody per unit time and per unit area is proportional to the fourth power of the temperature.

2.2 Thermal image analysis

It is necessary to distinguish between heat transfer. It should be distinguished whether it is heat transfer by reflection from other heat sources or radiant heat transfer by self-energy transfer. In other words, thermal image analysis must accurately confirm emissivity. Emissivity is the rate at which energy is radiated from a material, and since there is no ideal black body in reality, all of the thermal energy is not absorbed (A), and some of it is reflected (R) or transmitted (T), as shown in Figure 9.

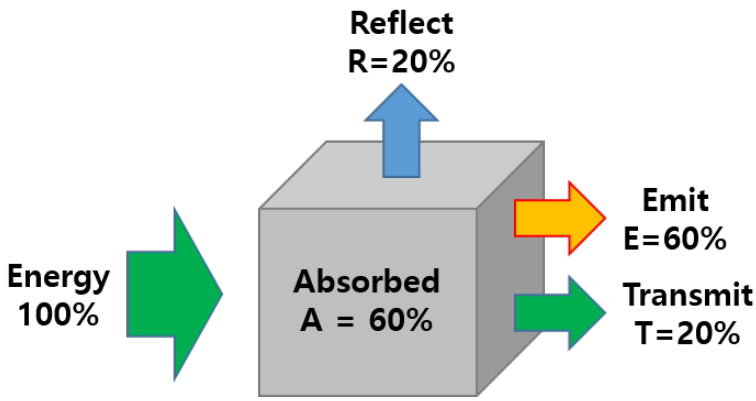

Figure 9: Emissivity of the object.

The actual object's temperature is 100°C, but when read with an infrared camera, it reads as 90°C, requiring 10% correction. At this time, the emissivity of this object is 90%. For accurate measurements with an infrared thermometer, you need to know exactly what the emissivity is. Since the emissivity of each material is different, each must be corrected when measuring and analyzing infrared temperature. Since emissivity and reflectance are inversely proportional, low emissivity means high reflectance. This is close to the apparent temperature of the surrounding object.

For checking the condition of electrical equipment in the study [15], we found the most suitable method based on image metrics such as MSE, PSNR value, Sobel and Otsu method. The thermal image was converted to an HSI color model, and the hot regions of the image were identified using gradient-based edge detection by Prewitt, Roberts, Sobel et al. For human acquisition, HSI model is more exact than RGB model [16].

$$H \simeq \begin{cases} \theta & \text{if B} \leq \text{G}\,, \\ 360 - \theta & \text{if B} \geq \text{G}\,. \end{cases} \tag{2.2}$$

In the HSI model, Hue(H) is measured in red.

$$S = 1 - \frac{\text{R} + \text{G} + \text{B}}{3} \min(\text{R,G,B})\,, \tag{2.3}$$

where Saturation(S) is obtained as the distance on the axis.

$$I = \frac{\text{R} + \text{G} + \text{B}}{3}\,, \tag{2.4}$$

where Intense(I) is the average of RGB.

Image metrics-based methods such as mean squared error (MSE) and peak signal-to-noise ratio (PSNR) have been proposed as the best method for thermal image processing.

$$MSE = \frac{1}{n} \sum_{t=1}^{n} e_t^2. \tag{2.5}$$

The simplest and most widely used quality metric is the mean squared error (MSE). It is calculated by averaging the difference between square values of the threshold image and the reference image pixel.

The PSNR depends on the MSE value. $x(i, j)$ is the original image, and $y(i, j)$ is the threshold image. M and N are the height and width of the original image, respectively.

For edge detection, the MSE value should be large and the PSNR value

should be small [17]. By this criterion, of the three methods, the Sobel method is most suitable for thermal image analysis. In addition, the otsu threshold method provides better segmentation results than the standard gray scale approach, so it is applied to find the hottest part of the thermal image.

2.3 Rule-based object detection

2.3.1 SIFT

For image comparison, it is possible to compare whether or not the image is the same only when the conditions in which the image was created are the same. However, even with the same image, the difference due to the difference due to the illuminance and the angle cannot be confirmed by a simple computer vision comparison method. Accordingly, a method of extracting and comparing features of images was devised.

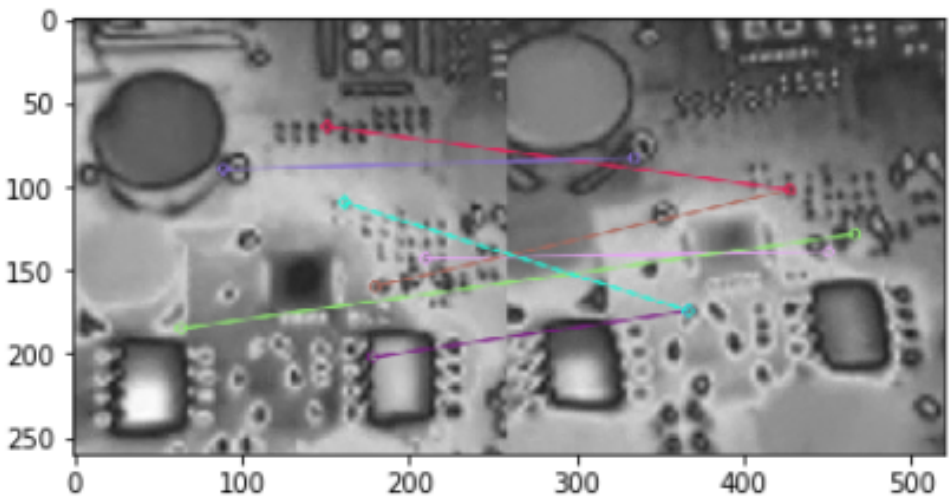

Figure 10: SIFT

Scale-Invariant Feature Transform(SIFT) [18] is an algorithm that extracts features that do not change even with size change and rotation. The principle is that after extracting SIFT features from two other images, matching similar features can find the corresponding part shown in Figure 10. It goes through 4 steps of Scale Space Extrema Detection, Keypoint Localization, Orientation Assignment, and Keypoint Descriptor.

In the Scale Space Extrema Detection step, the size of the original image is enlarged and reduced, and each changed image is gradually blurred. The Gaussian operator and the image can be convolved to blur. This step was applied to capture the difference in image clarity and size according to distance as Equation (2.6). Where G is Gaussian function and I is 2D image.

$$L(x,y,t) = G(x,y,t) * I(x,y). \tag{2.6}$$

Difference of Gaussian(DoG) operation is performed to find the keypoint of the image. Two adjacent blurred images of the same octave acquired in the previous step are subtracted.

In the Keypoint Localization step, the minimum and maximum values are found using three DoG images of the same octave in order to find the feature points. Compared with 26 pixels surrounding one pixel, if the minimum or maximum values are used, the feature points becomes keypoint. Among the many keypoints, those with low contrast and those that exist on the edge are removed because their utility value is reduced. Feature point selection is per-

formed to find feature points located in corners with relatively large changes.

In the orientation assignment step, orientation is assigned to feature points having scale in-variance to give rotation in-variance. A window is created at the feature point, and Gaussian blur is applied to obtain the gradient direction and size of all pixels in the window.

In the Key point Descriptor step, special information such as fingerprints is given to each feature descriptor. The characteristics of each key point are expressed as 128 numbers. To solve the rotation dependence problem of 128 feature vectors, the direction of the key point is subtracted from each gradient direction. Also, in order to solve the brightness dependence, normalization is applied.

2.3.2 PSNR and SSIM

PSNR [19] is used to evaluate loss information about the quality of an image generated or compressed in an image or video field. It represents the ratio of noise to the maximum signal that a signal can have. It is in decibel [db], and the smaller the loss, the higher the value.

For the evaluation of image quality, we tried to compare numerically, but to evaluate the image quality from the same perspective as the human eye, we applied SSIM (Structural Similarity Index Map) [20]. The human visual system is based on images. Since it is specialized in deriving structural information, the degree of distortion of the structural information has the greatest effect on the perceived quality.

Compare the brightness(2.7), contrast(2.8), structure(2.9) of the original

image x and the distortion image y. Where l is the Luminance, c is the Contrast and s is the Structure. And, μ is the mean, σ is the standard deviation and σxy is the cross covariance function.

$$l(x,y) = \frac{2\mu_x\mu_y + C_1}{\mu_x^2 + \mu_y^2 + C_1}, \tag{2.7}$$

$$c(x,y) = \frac{2\sigma_x\sigma_x + C_2}{\sigma_x^2 + \sigma_x^2 + C_2}, \tag{2.8}$$

$$s(x,y) = \frac{\sigma_{xy} + C_3}{\sigma_x + \sigma_y + 3}, \tag{2.9}$$

$$SSIM(x,y) = \frac{(2\mu_x\mu_y + C_1) + (2\sigma_{xy} + C_2)}{\left(\mu_x^2 + \mu_y^2 + C_1\right)(\sigma_x^2 + \sigma_y^2 + C_2)}. \tag{2.10}$$

The SSIM value can be modified mathematically with the PSNR value [21]. PSNR is more sensitive to additive Gaussian noise than SSIM. In addition, PSNR and SSIM are more sensitive to additive Gaussian noise than Gaussian blur, jpeg, and jpeg2000.

2.4 Deep learning analysis

2.4.1 CNN

Convolution Neural Network(CNN) is a convolutional neural network, which was introduced to effectively process images by applying filtering techniques to artificial neural networks. This is to automatically learn each filter element represented by a matrix suitable for data processing. The neural network is composed of an input layer, a hidden layer, and an output layer. The output is predicted by feeding forward through the input layer and the hidden layer to the final output layer. The cost function is calculated from the difference between the predicted value and the label of the input data. By applying the gradient method to the cost function, back-propagation to the input layer is obtained. Through this, the weight of each layer is repeatedly updated.

Filters, channels, and pooling exist in convolutional neural networks. Filter extracts the features of an image and improves accuracy. Filters can be automatically created and used. There are three RGB channels in one color, and in order to reduce an error, there are many cases that the image is changed to black and white and used as one channel in the pre-processing process.

To reduce the dimension and maintain information, a pooling technique is applied. For pooling, average pooling and max pooling are used. Average pooling is a method of having the average value of the filter as a feature when an image is characterized by a filter. Maximum pooling is a method of characterizing the maximum value of the filter. Maximum pooling is more used to show the distinction and change of features well, and to facilitate neural

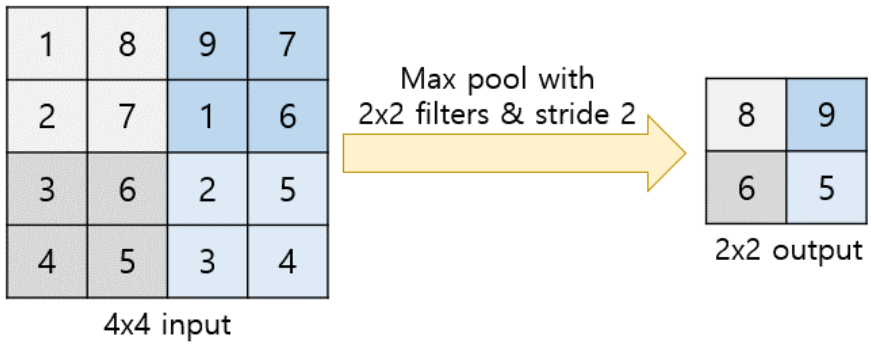

Figure 11: Max pooling

network learning ah shown in Figure 11. After convolution activity by filter, many features are made on convolution layer. Because of many features, overfitting is happen. By reducing the number of features through pooling, overfitting does not occur.

Table 5: CNN Model

CNN models
1. Lenet : Yann Lecun, 1990s [22]
2. Alexnet : Alex Krizhevsky, 2012 (Winner of ILSVRC 2012) [23]
3. Googlenet : Szegedy, 2014(Winner of ILSVRC 2014) [24]
4. VGGNet : Karen and Andrew, 2014(2nd of ILSVRC 2014) [25]
5. Resnet : KaimingHe, 2015(Winner of ILSVRC 2015) [26]

Representative CNN models are Lenet, Alexnet, Googlenet, ResNet, and VGGNet. Lenet [22] is a structure that can recognize handwritten characters using CNN. It consists of a total of 7 layers. Alexnet [23] consists of 8 layers, 5 convolutional layers and 3 fully connected layers. Relu was first applied as an activation function. Googlenet [24] proposed a structure that can improve efficiency by reducing the number of parameters while improving

performance by keeping the neural network deep. Inception, a neural network module concept, was presented. VGGNet [25] increases the depth of the network through a small 3x3 filter, and the number of channels increases as the layer gets deeper. As the layer gets deeper, problems such as gradient vanishing and exploding occur. To prevent this, ResNet [26] proposed skip connection in Figure 12. Skip connection make model more deeper layer.

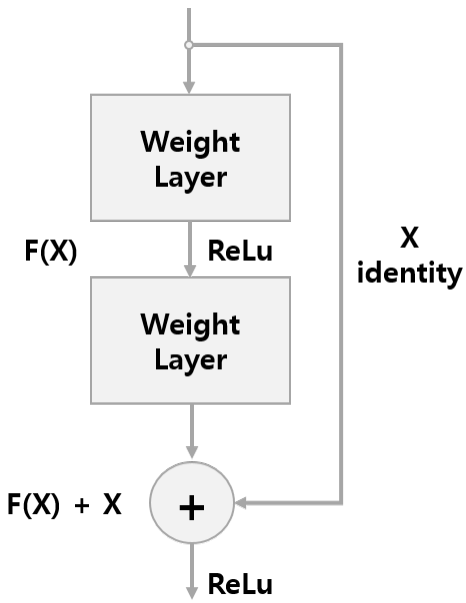

Figure 12: Skip connection.

VGGNet [25] is a model that won second place in the 2014 ImageNet image recognition competition. VGG19 refers to a model composed of 19 layers. Starting with the VGGNet model, the depth of the network began to deepen a lot. The 2012 and 2013 championship models consisted of 8 floors, but in 2014 VGGNet (VGG19) will have 19 floors, GoogLeNet will have 22 floors, and 2015 ResNet will have 152 floors. Through this, it can be seen

that the more layers of the network and the deeper the better the performance. VGGNet has a simple structure, easy to use, and excellent performance, so it was applied to this study.

VGG16 has 16 convolution layers and dense layers. To check only the effect of depth, the size of the convolution filter was fixed at 3x3. Because the filter size was small, the image could not be rapidly reduced and the depth of the network could be deepened. Convolution three times with a 3x3 filter yields a feature map of the same size as one convolution with a 7x7 filter. Also, the number of parameters has been reduced. A 3x3 filter generates a 3x(3x3)C2 = 27C2 parameter, but a 7x7 filter creates a (7x7)C2 = 47C2 parameter, which can reduce parameters by 81 percent. Also, as the layers are stacked, the nonlinearity increases, so the properties become more and more useful. By applying VGG16 as the basic network, Cang zhang conducted a study to discover 6 PCB defects that occur during the PCB manufacturing process [27].

2.4.2 AutoEncoder

CNN-based networks such as VGG16 apply supervised learning, which repeatedly learns through a lot of data. However, when the number of data is small and there is difficulty in supervised learning, an unsupervised learning method is applied.

AutoEncoder [28] is characterized in that it learns each layer of a neural network step by step and reproduces input data in the final output. The number of input and output nodes is the same, but the number of nodes in the

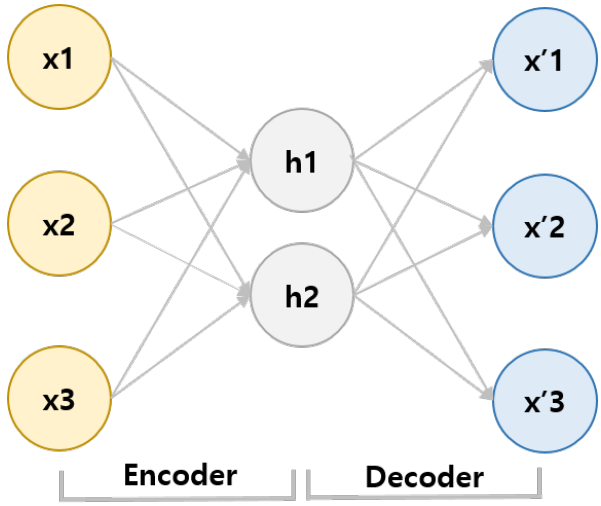

Figure 13: AutoEncoder.

hidden layer is less than the number of input/output nodes. The input data is compressed in the hidden layer to extract features, and the input data is reproduced based on the extracted features. Learn to restore compressed data and noise-added data. Learn how to express efficiently, not just output for input.

In order to detect defects in the PCB itself, Khalilian [29] proposed the Denosing Convolutional Autoencoder method. Defective image with salt/pepper noise and normal image are entered into the autoencoder together to train model. When a test image is applied to the trained autoencoder, a signal-processed image is generated. By finding a defect based on the difference between the test image and the generated image, it is determined whether it is normal or defective. It has 97.5% accuracy and shows higher performance than other existing algorithms.

2.4.3 One-shot learning

In order to configure a system for object classification, sufficient data on an object is required, and when a new classification is added, it is difficult to newly learn a network. However, it is difficult to obtain sufficient data in reality, and it is possible to face the problem of classification that has not been learned. To solve this problem, one-shot learning or few-shot learning methods were devised. This is a method of predicting which classification the test object is through one or several classification learning [30].

Siamese Network takes two images as inputs, vectorizes them, and expresses the degree of similarity between the two vectors. If it is equal, it represents 1, and if it is different, it represents 0. The Siamese network has a weight shared between two images, and transforms the image into a vector through a convolution operation. Normally, L2 distance is used, but the similarity is measured with Weighted-L1 Norm. Cross-entropy used in Siamese networks is used, and similar images have a close distance, and other images have a long distance, and metric learning is performed.

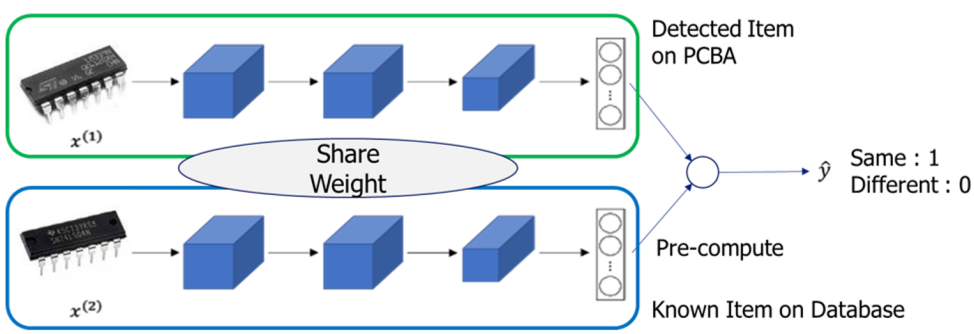

Figure 14: Siamese Network

In order to check the defects of electronic components in the electronic product manufacturing process, deep learning technology is being used. There is a report on whether it is defective or normal by comparing the image of the component applied on the PCB with the image of the known component [31].

To check the similarity of the image, a Siamese network was used as shown in Figure 14. When a component image (x(1)) on the PCB is input and image vectorized through the shared weight, the normal component image is vectorized. Compare with the data to measure the degree of similarity. By comparing the network based on AlexNet and VGG16, it was shown that the network based on VGG16 is better. In addition, the method of optimizing the entire layer with IC image showed good results compared to the method of optimizing only some layers with 92.31%.

Chapter 3

Problem definition and proposed methods

In this chapter, the problem to be solved in this study is clearly defined, and the scope of the study and the solution to the problem are explained. In order to detect PCBA defects that do not appear externally, a thermal imaging test, a non-contact method that can replace the existing in-circuit inspection method, was proposed. The problem to be solved in this study is defined, and a brief overview of the solution is provided.

	Vision Test	IR Test
Reference Sample	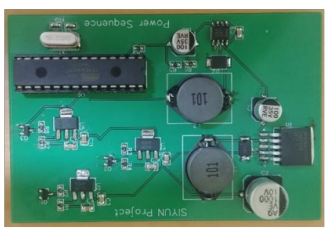	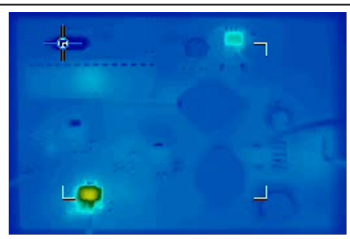
Test Sample		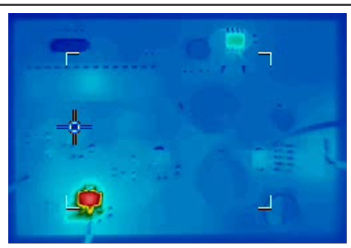
Compare	Same (OK)	Different (NG)

Figure 15: Vision Test vs IR Test

3.1 Problem definition

PCBA defects are confirmed through image comparison and deep learning analysis of the thermal image obtained through the thermal imaging test, which is a non-contact method. The goal of this study is to design an optimal model for image analysis to maximize accuracy. Our goals are presented as follows.

$$\text{Accuracy: } \max_{f} A(f) > 90\%, \tag{3.1}$$

$$\text{SSIM: } \max_{f} S(f) > 0.9, \tag{3.2}$$

$$\text{Test Time: } \min_{f} T(f) < 30sec, \tag{3.3}$$

$$\text{Image: } 1 \leq f \leq 3000. \tag{3.4}$$

Where $A(f)$ is the defect detection accuracy when a defective image is input f. And, $S(f)$ is the SSIM, $T(f)$ is the Teset time. Accuracy is defined as the criterion that can better discriminate defects and good products among PCBA thermal image data. In some cases, there may be a case of non-probation that identifies a defective product as a good product, and a case of a false detection that determines a good product as a defect may occur. Comprehensively judged by accuracy, and expressed as equation 3.5 based on confusion matrix in Table 6 [32].

$$Accuracy = \frac{\text{TP + TN}}{\text{TP + TN + FP + FN .}} \tag{3.5}$$

Table 6: Confusion Matrix.

Division		Prediction	
		Positive	Negative
Actual	Positive	True Positive(TP)	False Negative(FN)
	Negative	False Positive(FP)	True Negative(TN)

The image analysis optimization model is aimed at maximizing accuracy and has an accuracy of more than 90%.

3.2 Proposed methods

For the analysis of PCBA thermal images, the traditional image analysis method and the deep learning image analysis method are applied together and reviewed. By applying the previously reviewed SSIM, CNN, RCNN, and AutoEncoder methods, thermal images are analyzed and compared, and a method suitable for the production environment is presented.

3.2.1 Rule based method

To find defects, the normal thermal image and the defective thermal image are directly compared. The structural similarity that measures the image quality is measured through SSIM, not a direct comparison of the image pixels themselves. SSIM evaluate the visual impact of the three characteristics of an image which are luminance, contrast, and structure.

First, the images are compared with the camera fixed at the saturation

temperature. By comparing the images measured at the same position and angle, it is possible to check whether or not there is a defect, and further, by dividing the comparison area and measuring, the area where the defect exists can be identified.

Additionally, experiment is executed with data rotated 5 degrees and 10 degrees of the camera's measurement angle. Considering the vibration of the production line and changes in the environment, check whether the SSIM method is applicable. The normal and defect images obtained from free camera angles are compared with each other to see whether it is possible to confirm the defect.

3.2.2 Deep learning based method

Deep learning-based technologies have recently been applied a lot such as Surface integration inspection, Machinery fault diagnosis, Predictive analytics and defect prognosis. In this study, a CNN-based deep learning model is applied to learn normal and defect images, and to identify defect images. The CNN model consists of 3 convolutional layers, 3 pooling layers, and 3 fully connected layers. Total number of parameters is 4,112,346. In consideration of the production environment, defect detection is attempted with images measured at various positions and angles under heat saturation. The optimizer applied Adam, trained with 500 epochs, and divided the training image by 7:3 to learn and evaluate.

Performance and application of the applied CNN model can be checked. The Tack time of the existing ICT method that detects defects is 30 seconds.

Through comparison with existing productivity, it is checked whether it is applied. At a fixed position and a fixed camera angle, thermal images are acquired every 10 seconds, and the trained model is tested to see if there is any defect. After confirming the time that can be distinguished, the camera measurement angle is adjusted to obtain data corresponding to the production environment. Finally, check whether the thermal image is defective through supervised learning and the applicable environment.

RNN method is applied to check if it is possible to detect defects. AutoEncoder method is also applied to a fixed normal image to check if it is effective in unsupervised learning. After entering the reduced image and the original image, the relationship between image quality and defect detection was checked. The similarity to the original image is checked through SSIM, and if the SSIM is 0.9 or higher, it is judged as the same normal image as the original image.

Recommended method is different with existing research [6] as shown in Table 7. Defect is measured on area not point. If component value is different with original value, defect area has different thermal image pattern. For example, when resistor value for MAX15023 DCDC converter frequency setting is changed, temperature of another part is changed.

Table 7: Different method for thermal test.

	Existing	Recommended
Test Approach	HW component	HW + SW
Test Area	Defect point	Defect Area
Measured Data	Temperature(Text)	Thermal Image
Analysis Method	Mathematical(MSE)	Probabilistic comparison

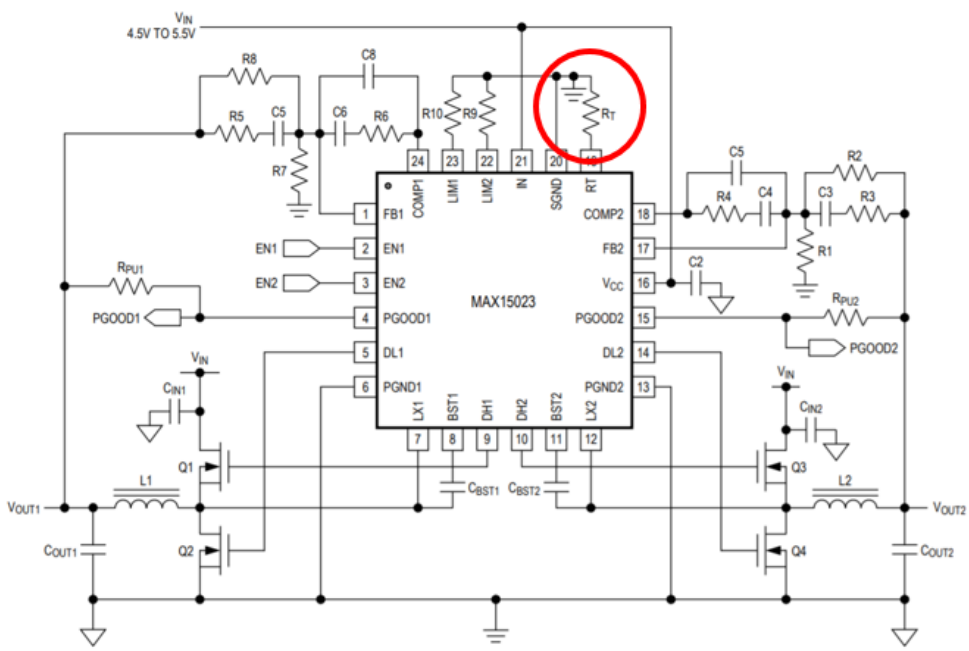

Figure 16: Frequency resistor change : 40kohm to 20kohm.

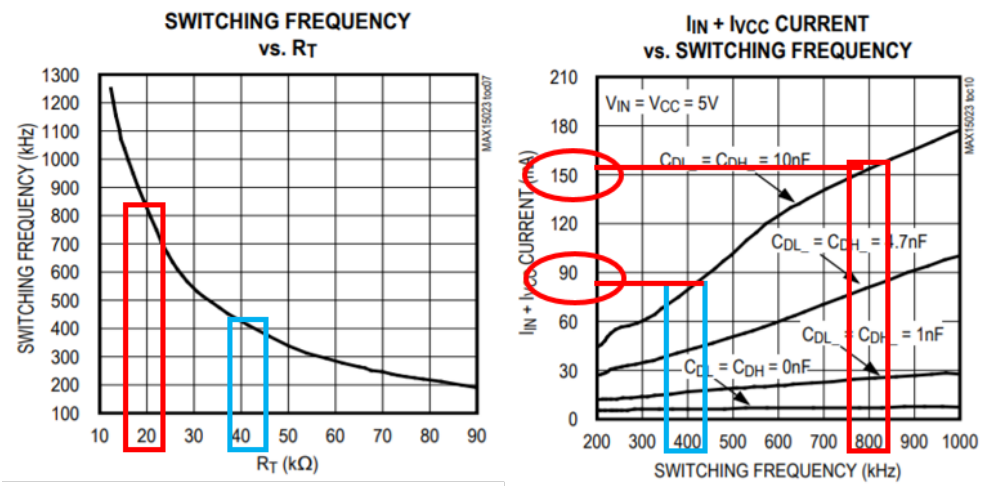

Figure 17: Setting Frequency and current consumption change.

Chapter 4

Experiment and evaluation

Briefly explain the thermal image for image analysis, and conduct a related image experiment. In the first experiment, the traditional image comparison method is applied to find defects, and accuracy according to data types is checked and analyzed. The second is to find defects by applying several deep learning methods, and to check and analyze the accuracy according to the data type. Finally, the accuracy is checked by applying the ensemble method that combines the two methods.

4.1 Dataset definition and construction

Thermal images were acquired using a PCBA manufactured in the field. The PCBA was positioned and the thermal imaging camera was fixed or moved freely to acquire image data. The thermal imaging camera was FLIR's T420 model, which was able to acquire a 320 x 240 resolution thermal image. The thermal image at the fixed position was measured with the thermal imaging camera fixed as shown in Fiture 18. Using a PCBA fixture, a PCBA thermal image was acquired in a fixed state, and a non-fixed thermal image was acquired by moving the camera freely while the PCBA was positioned. A fixed thermal image dataset and a free thermal image dataset were acquired.

The static thermal image is a dataset used in traditional vision tests. Var-

ious image sets were acquired for comparison between the deep learning image analysis method and the traditional vision analysis method, and a transient thermal image was also prepared for failure analysis through thermal diffusion over time.

Figure 18: Test environment for thermal image acquisition.

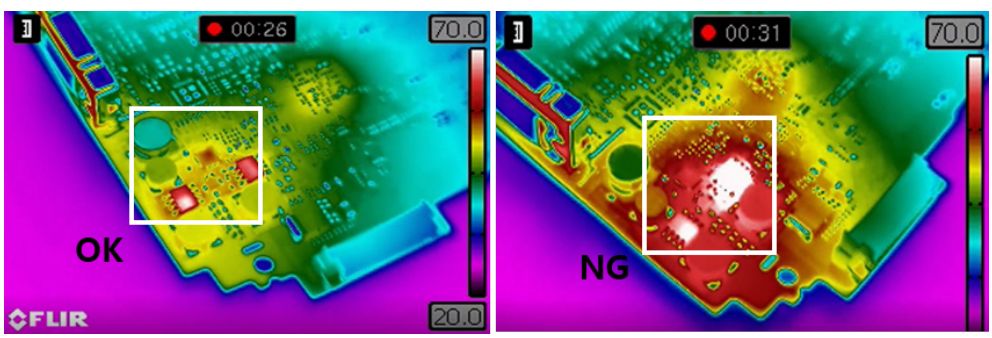

Figure 19: Thermal Image by thermal imaging camera.

The thermal image was recorded in a video file format, and the parts necessary for the test were acquired as images in Figure 19. The image is composed of a size of 260x260 at a free angle under heat saturation, and is normal. And 500 images of each of the defective images were prepared by increasing the data. For data increase, only the Rotate and Flip methods were applied, and the images were increased by 100 each with 90°/270° rotation and vertical/horizontal fold methods.

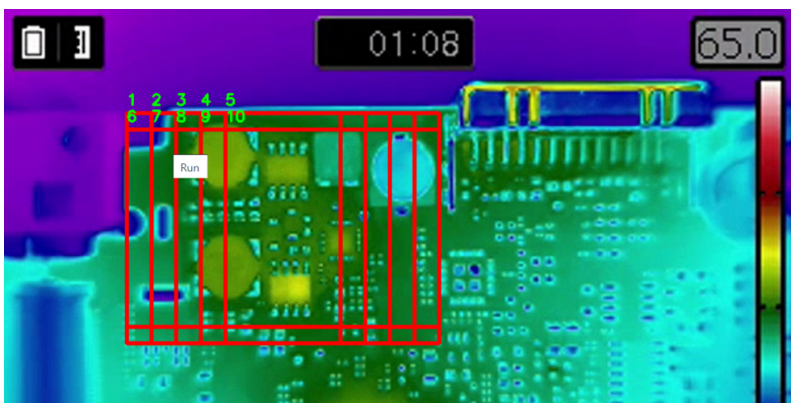

Figure 20: Image extraction by time.

In order to check the suitability for application in the production process, 30 images were extracted at 10-second intervals in the fixed state and the thermal transient state, and 10 different positional images were acquired each in Figure 20. Time A total of 600 images were prepared for each time period in order to check the analysis ability over time. In addition, in order to check the accuracy according to the camera angle, the 5° rotation image and the 10° rotation image were increased by 1200 sheets each time. The dataset prepared for all tests is shown in Table 8.

Table 8: PCBA Thermal image Dataset.

No	Image Dataset	OK	NG
1	Saturation, Free angle	500	500
	Saturation, Fixed angle	500	500
2	Transient(10s),Fixed angle	300	300
	Transient(20s),Fixed angle	300	300
	Transient(30s),Fixed angle	300	300
	Transient(40s),Fixed angle	300	300
3	Transient(30s),Rotation (5°, 10°)	1200	1200
	Transient(40s),Rotation (5°, 10°)	1200	1200

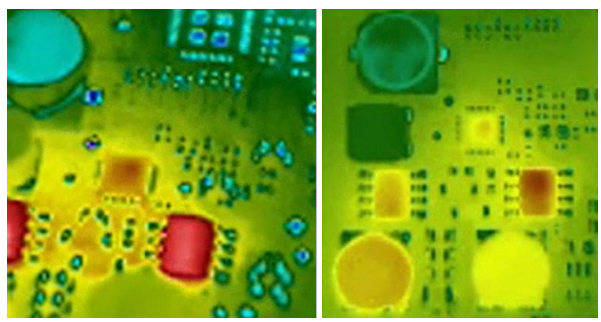

Figure 21: No.1 - Free angle, Fixed angle.

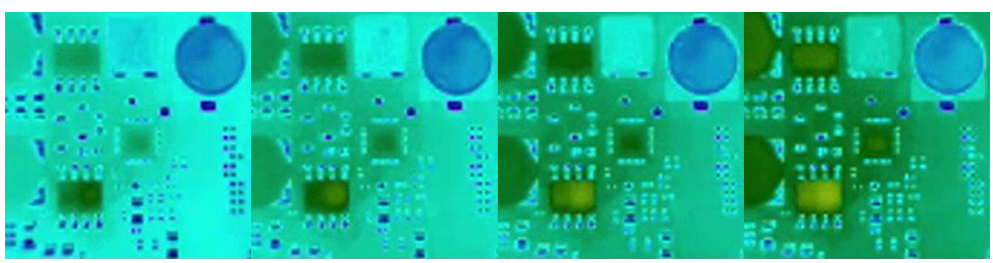

Figure 22: No.2 - Transient 10s, 20s, 30s, 40s.

Dataset can be divided with 3 case. First, Saturation dataset is used for AutoEncoder Method test. After PCBA is saturated, thermal image was measured. Second, Transient Fixed dataset. These are used for testing productiv-

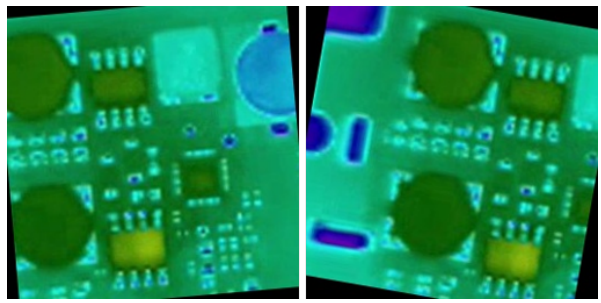

Figure 23: No.3 - Rotation ±5°, ±10°.

ity according to power input time. Third, Camera angle is different. Considering production environment, measured angle is changed.

4.2 Progress and results

4.2.1 SSIM

Thermal images were analyzed using SSIM, a structural similarity index that measures image quality. Thermal images were compared in a stable state, which is a temperature saturation state. If a thermal image of the same pixel is received and analyzed through a fixed measurement environment, a defective image can be easily found.

If there is a difference of 5% or more by measuring the SSIM in the normal state through the reference image and comparing it with the SSIM value in the normal state, it may be determined as a defect. By classifying the test image and measuring the SSIM for each measurement area, detailed defect areas can be identified. As shown in Figure 24, defects can be easily identified by comparing images of the same pixel area, and further, defective

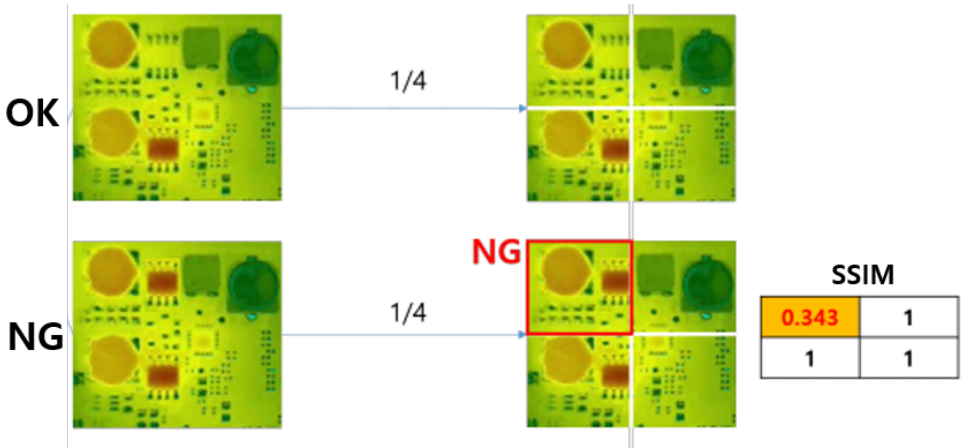

Figure 24: Image comparison with SSIM.

areas can be identified.

Although defects can be checked with a simple method, the SSID comparison method alone has limitations because the measurement environment is not always the same. Images in the free-angle state were compared with each other. Although the images are the same object, the structural similarity was measured low because the viewing angle and height were different.

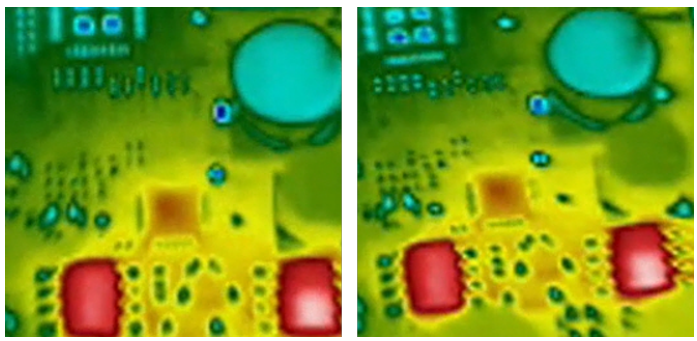

Figure 25: Disadvantages of SSIM.

In the case of Figure 25, the thermal images of the same object were

compared in the thermally included state, but the SSIM was measured as low as 0.248 due to the small difference in measurement position. Since SSIM compares the pixels of the same location of two images, it is difficult to apply to image quality comparison unless the image is the same. Moreover, it is difficult to obtain a constant image because it is always fixed in places with a lot of vibration such as a production line.

4.2.2 CNN

When comparing images using SSIM, defects can be easily identified, but a small difference between the measurement angle and measurement area makes it difficult to find defects as shown in Figure 25. SSIM measurement value is 0.248 between similar images. A method to cope with these difficulties is a deep learning analysis method using CNN. You can find defective products by learning genuine products and defective products in various conditions. PCBA is operating and thermally saturated steady state images were prepared for each of 500 normal/defective images. Thermal images were acquired from various angles and heights. Thermal images were acquired with defective products due to mis-interpolation of parts and application of this product, and labeling was performed only as normal and defective like as Figure 26.

The defective thermal image (Label:1) and the normal thermal image (Label:0) were divided by a ratio of 7:3, and 70% were used for training and the remaining 30% were applied to the test. The CNN model used at this time is shown in Figure 27. The original image is 260x260, but I resize it to

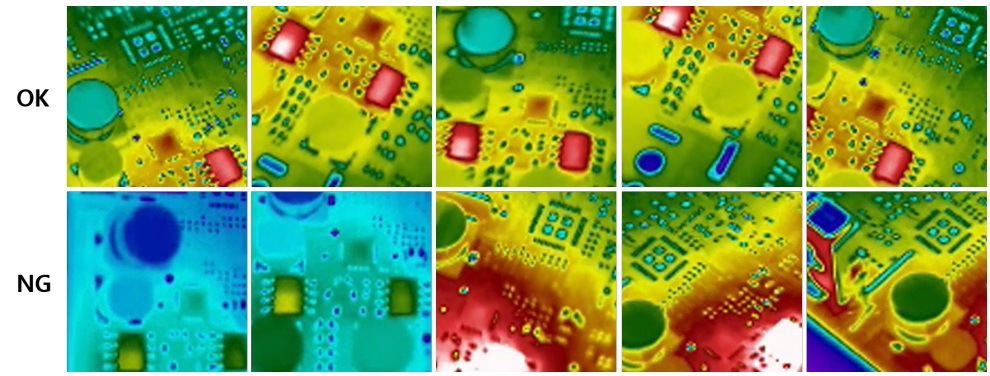

Figure 26: CNN Test Dataset.

64x64. In order to maintain the color information of the thermal image, gray conversion was not performed and RGB characteristics were maintained. It consists of a simple three-layer convolution layer and a max pooling layer, and a fully connected layer and dropout are applied. For max pooling, 2x2 filter and 2 stride were applied.

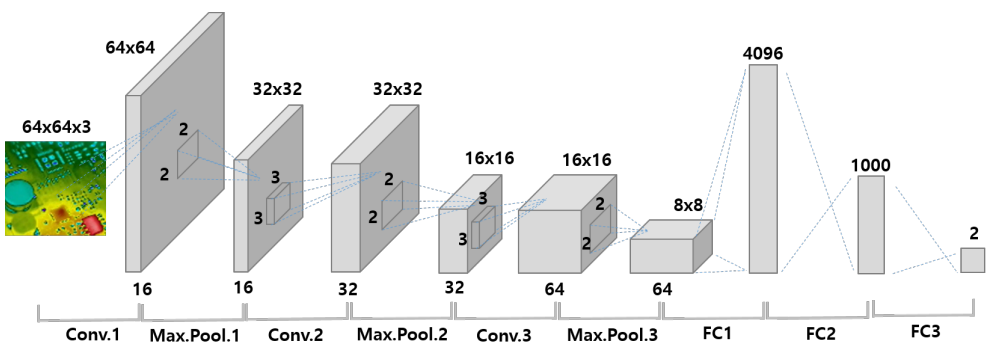

Figure 27: CNN Model.

By applying 128 batches and 500 epochs, 840 images were trained and 160 images were tested. The final test loss was 0.023 and the test accuracy was 0.9916. For the thermal image with normal and bad labeling, defects could be

detected with an accuracy of more than 99%. One image was normal, but there was a mistake that was judged as bad. Through this experiment, it was found that defects can be found through supervised learning of thermal images.

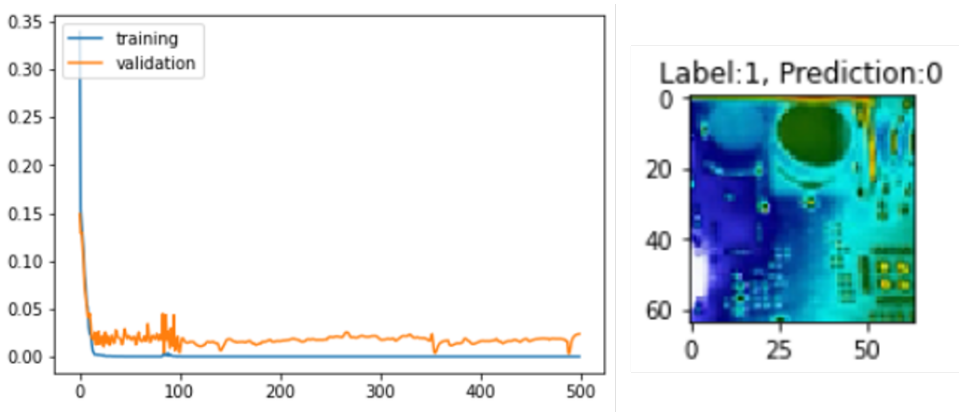

Figure 28: CNN result

However, since the thermal image used in the experiment is an image measured after applying power and heat saturation for 2 minutes, it is difficult to apply it in a factory where productivity is important. In the case of detecting a defect with the existing ICT method, it took 30 to 40 seconds to test one PCBA. In order to check the applicable time in the current test PCBA, the thermal image was classified at 10 second intervals after the power was applied. Images were extracted by dividing into 10 different location images, and 600 images were constructed by combining normal and defective images.

By learning the image dataset by time and measuring the defect detection accuracy with the CNN model, meaningful results were obtained 30 seconds after the power was applied With an accuracy of 96.6%, it was able to distinguish between genuine and defective products. After 40 seconds of power on,

the thermal distribution of the image was clearly different, so 100% defective products could be identified in Figure 29.

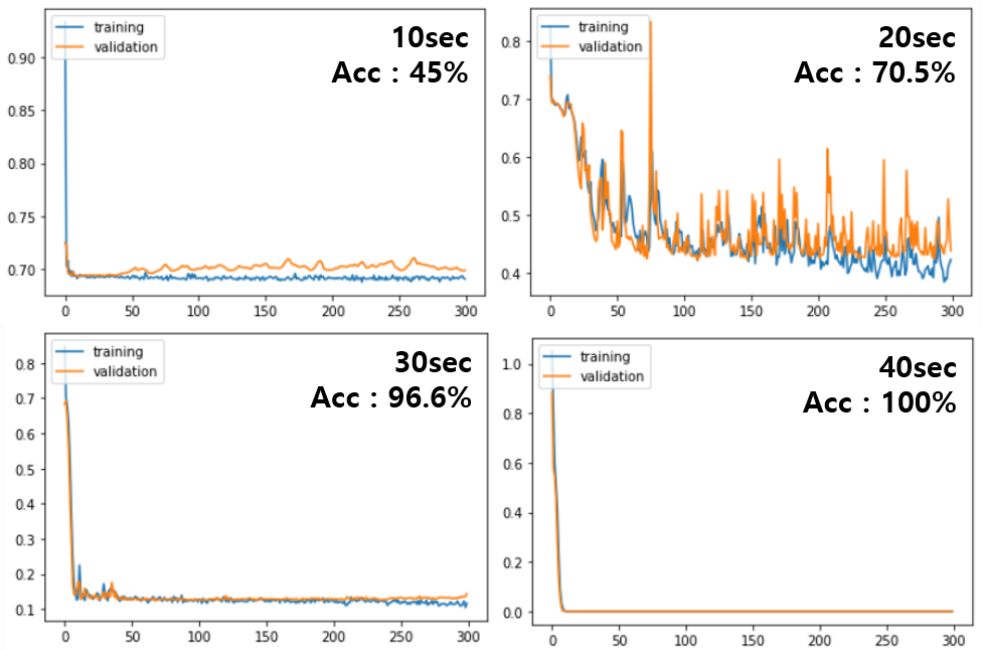

Figure 29: Accuracy in power-on time.

Although the thermal imaging camera was fixed on the production line, the camera could change the angle by 5° or 10° due to mechanical vibration, so the rotation image was increased by 1200 images in the 30-second thermal image to learn and learn about defects and normals. It had a defect detection accuracy of 96.6% in 600 fixed images, but with the addition of 5° and 10° rotated images, it was possible to obtain a result that was 2.6% less accurate. As the epoch increased, over-fitting occurred and the error rate of the verification step increased in Figure 30.

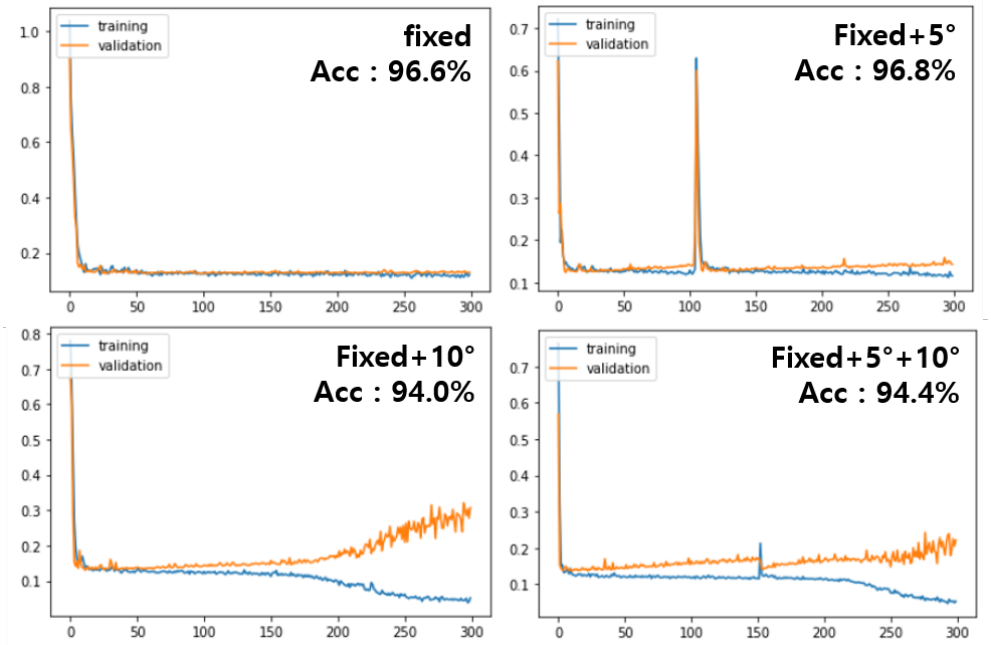

Figure 30: Accuracy on camera angle.

4.2.3 RCNN

It was possible to classify whether it was bad or not through CNN supervised learning. Furthermore, to determine where these defects exist, There are several ways for object detection. Object detection is on development from RCNN [33], Fast-RCNN [34], Faster-RCNN [35], Mask-RCNN [36] and YOLO [37]. we applied RCNN. RCNN is a method that extracts a region with 2000 features from an input image using a selective search method [38] and classifies it by applying it to a pre-trained CNN model. We applied the existing CNN model that learned the normal and the bad in advance.

Using RCNN's region proposal, regions with 2000 features were created, but the proposed region in the PCBA thermal image did not have any special

meaning. Accordingly, it was set to propose an area having an area of a certain size or more. The classification time was shortened as the proposed area was reduced to 50 like as Figure 31.

Classification was performed through the CNN model that trained the proposed region, but the results were not displayed like as Figure 32 Thermal images do not have special features because they judge the overall temperature distribution of the part. Since it is a classification that checks the temperature difference of the relative heat distribution, classification and location detection through RCNN was not possible.

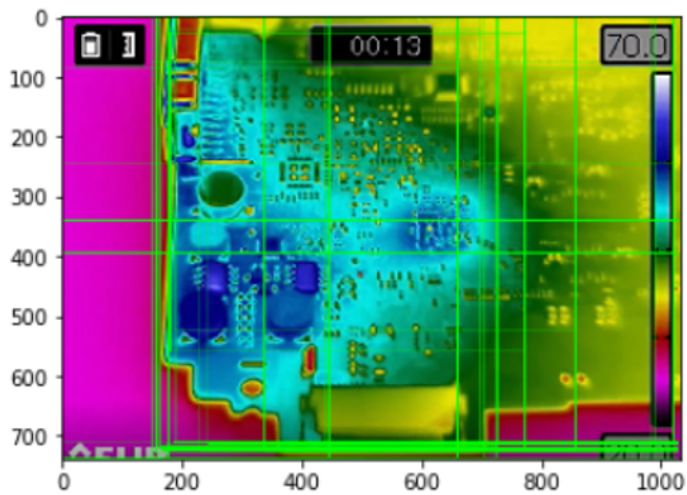

Figure 31: Region proposal with 50 area.

4.2.4 AutoEncoder

For the thermal image generated in the process line, labeling individually brings a lot of loss in terms of workability and productivity. Therefore, we apply a method that can quickly determine defects without performing addi-

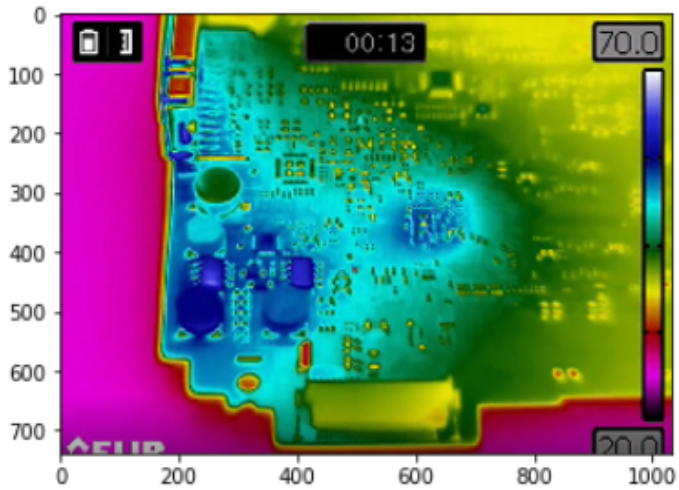

Figure 32: Test Result with RCNN.

tional labeling work. Since the AutoEncoder method is unsupervised learning, it is a learning method that extracts features of input data through an encoder and reconstructs original data through a decoder.

AutoEncoder was tested by applying thermal images of 500 regular products that were applied to CNN. An image of 260x260 size was adjusted to 28x28 size and input, and 500, 1000, 2000, 3000, 4000 and 5000 times were learned, but the shape of the reproduced image was unknown like as Figure 33.

Even if the input thermal image size was input as the original image size of 260x260 size without adjustment, the same result was obtained. The AutoEncoder result according to the input image quality did not change. Even if the image quality is high, it is difficult to find the same features in various images like as Figure 34.

It can be seen that rather than being affected by the quality of the input

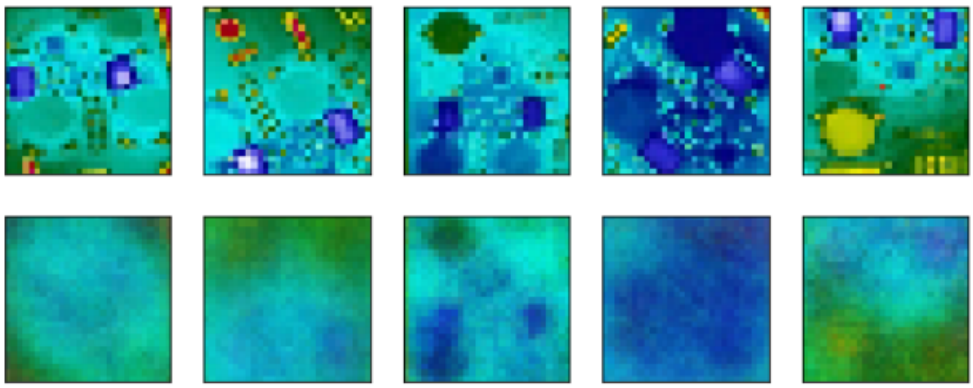

Figure 33: AutoEncoder Test: Resized image input.

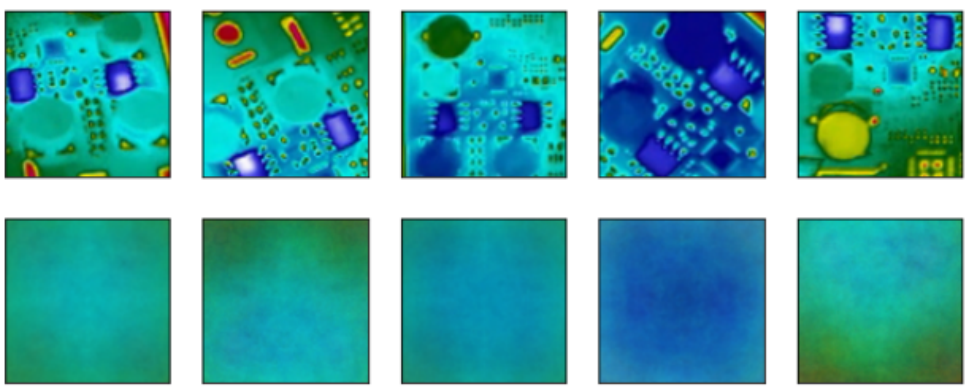

Figure 34: AutoEncoder Test: Original High-Quality image input.

image, images that can represent features are needed. Since it is impossible to cope with images measured at various angles and heights, a fixed measuring device was used to apply a thermal image of a certain area at a certain height. There was a positional error, but the features were well understood and the image was reproduced. If you check the similarity between the test image and the generated image by applying SSIM, which is the image similarity, you can see 98.05% similarity such as Figure 35.

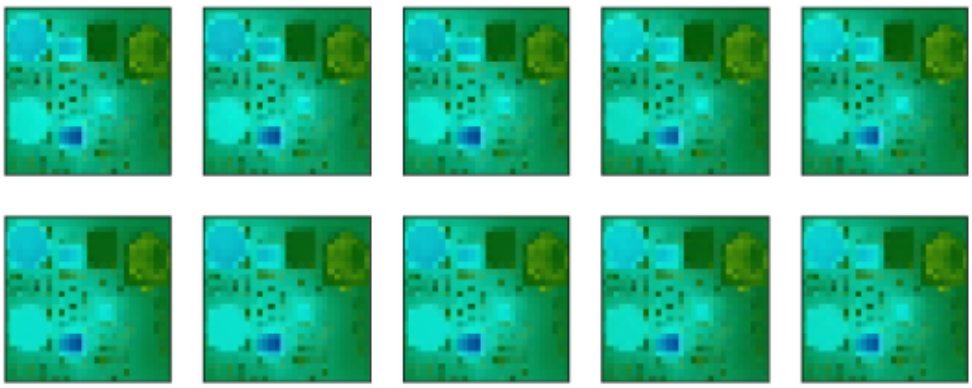

Figure 35: AutoEncoder Test: Fixed image input.

When learning with a normal image and inputting a defective image, a difference in similarity between the input image and the generated image occurs, so that defective products can be detected. When a normal image is input, the similarity is measured more than 0.97, but the defective product is measured less than 0.9 such as Figure 36.

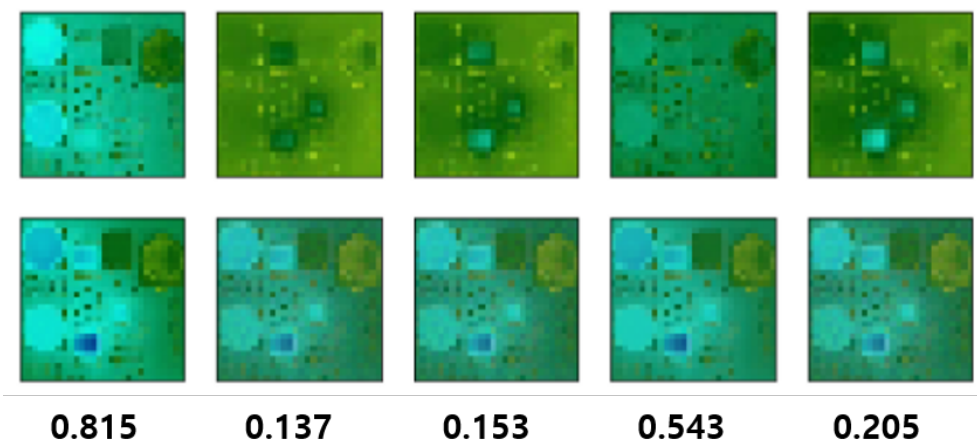

Figure 36: AutoEncoder Test: Defect detection.

Chapter 5

Conclusion and evaluation

5.1 Conclusion

The rule-based image comparison method can easily compare normal and bad images. However, even if the image is same, it cannot be applied to the production line because it has an error of judging a different image if the angle and position are changed.

Among various deep learning methods, when the supervised learning-based CNN model was applied, the defect could be effectively determined. When considering the production line environment and productivity such as vibration, it was possible to confirm defective products with thermal image data within 30 seconds after power was applied to the PCBA. This means a level of productivity similar to that of the existing ICT method. Although the accuracy of supervised learning was confirmed, it is difficult to apply it to defect detection of new products because a large number of defective images must be learned. In this case, the original product image is learned using the AutoEncoder method, which is an unsupervised learning, and defective products are detected through comparison with the generated image. Image comparison is quantified using SSIM, and if it is 0.9 or more, it is judged as the same image.

Table 9: Deep learning analysis method.

	Pros	Cons
SSIM	Fixed image test Defect Area	Fixture Cost increase
CNN	Productivity(30sec) High accuracy even in vibration	Data labeling
AutoEncoder	Fixed image test No need labeling	Fixture Cost increase

Through the research, it was confirmed that PCBA defect detection is possible through thermal images, and dataset of thermal images of actual mass-produced products were established. It raises the possibility of detecting PCBA defects through thermal images. It helps to detect defects by quickly discovering whether there is a defect, not a specific defect.

5.2 Lessons and Learned

Defect detection is possible through existing vision analysis for different shape parts mounting, parts not mounting, and parts information abnormalities on the PCBA. However, defects in the resistance value of a chip resistor of 1005 size or less, or a defect in the capacitance of a chip capacitor cannot be detected through vision analysis because it is impossible to analyze the external characteristics.

If it is not possible to detect external defects, the PCBA production process traditionally uses an ICT method to measure resistance values and capacitor capacity to find defective products. However, ICT has a problem that not

only gives an electric shock to the PCBA through a contact test method, but also has to secure an additional space for testing in the PCBA itself. In terms of productivity, there is also cost problem that the ICT test jig needs to be replaced periodically. In the electronics industry, where parts are shrinking and being integrated, it is no longer possible to detect defects using conventional methods.

Therefore, the proposal of this paper suggest the possibility to replace ICT and detect PCBA defects. Through deep learning, it was possible to learn the data of original and defective products, and check whether the input thermal image was defective. It was not possible to accurately determine the location of the defective product, but it was possible to find that the product was different from the normal.

For a product line that has been produced for a long time and has only a certain number of defects, it is possible to detect defective products at free and fixed angles by learning defective images through CNN. However, in a new product group or a product line that does not have a lot of defective data, an autoencoder is used to learn the original product, input the image of the product being produced, and the defective product can be identified through the reproduced image.

The traditional image comparison method is advantageous if an exact matched image can be continuously received using a fixed camera. Through simple image comparison such as XOR and SSIM, defects can be identified only by image differences. However, since it is difficult to extract a fixed image in a factory where there is a change in production environment such

as vibration, deep learning learning and defect detection methods capable of responding to image shaking are more useful methods.

5.3 Limitations of research and future research

For defects that are not apparently visible, thermal image analysis was applied based on the power circuit. This is because the power circuit is a part that supplies voltage and current, and it is easy to check the heat change by changing the resistance value. Deep learning thermal analysis limited to the power supply circuit was conducted, but additionally, an experiment is required by constructing thermal image data of the entire PCBA.

In this paper, data were secured and tested based on a specific PCBA, so the measurement results will differ due to changes in conditions such as circuit configuration and PCBA stacked structure. Since the experimental results were derived based on the PCBA applied in the experiment, it is necessary to construct a thermal image data set that can be applied to a general PCBA. For the detection of defects in PCBA that are becoming smaller and more integrated, I hope that the proposals in this paper can be practically helpful in production environments.

If a defect detection method using thermal images is applied to a smart factory, costs can be reduced because additional production facilities such that fixtures are not required. In addition, it can contribute to increase productivity, because of time savings in model change. After mass production, in order to check traceability, it is necessary to reinforce the production computer system

because images for each product must be stored.

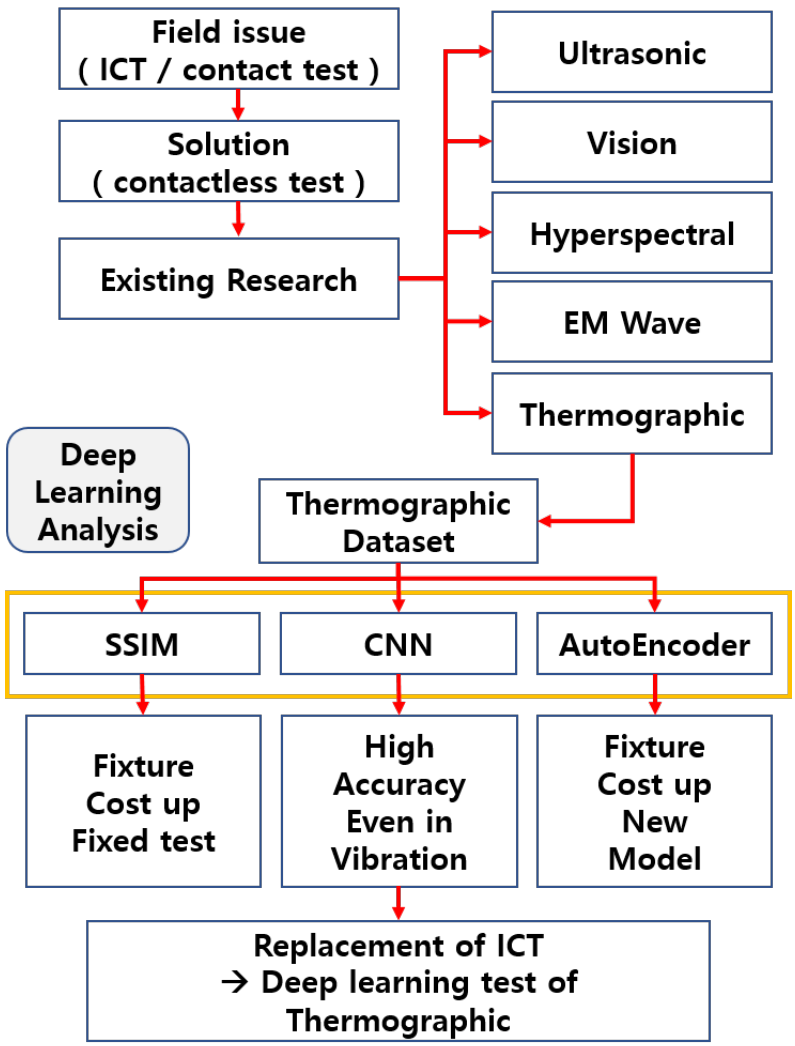

Figure 37: Project all flow

Bibliography

[1] C. Pramerdorfer and M. Kampel, "A dataset for computer-vision-based pcb analysis," in *2015 14th IAPR International Conference on Machine Vision Applications (MVA)*. IEEE, 2015, pp. 378–381.

[2] D. Anitha and M. Rao, "A survey on defect detection in bare pcb and assembled pcb using image processing techniques," in *2017 International Conference on Wireless Communications, Signal Processing and Networking (WiSPNET)*. IEEE, 2017, pp. 39–43.

[3] V. Ganavi and M. Rao, "Printed circuit board assembly defects detection using image processing techniques," *Int. J. Eng. Sci*, vol. 6, no. 6, pp. 7824–7829, 2016.

[4] N. E. B. Alaoui, P. Tounsi, A. Boyer, and A. Viard, "New testing approach using near electromagnetic field probing intending to upgrade in-circuit testing of high density pcbas," in *2018 IEEE 27th North Atlantic Test Workshop (NATW)*. IEEE, 2018, pp. 1–8.

[5] A. Renbi and J. Delsing, "Contactless testing of circuit interconnects," *Journal of electronic testing*, vol. 31, no. 3, pp. 229–253, 2015.

[6] N. E. B. Alaoui, P. Tounsi, A. Boyer, and A. Viard, "Detecting pcb assembly defects using infrared thermal signatures," in *2019 MIXDES-26th International Conference" Mixed Design of Integrated Circuits and Systems"*. IEEE, 2019, pp. 345–349.

[7] F. Al-Obaidy, F. Yazdani, and F. A. Mohammadi, "Intelligent testing for arduino uno based on thermal image," *Computers & Electrical Engineering*, vol. 58, pp. 88–100, 2017.

[8] A. A. Sarawade and N. N. Charniya, "Infrared thermography and its applications: a review," in *2018 3rd International Conference on Communication and Electronics Systems (ICCES)*. IEEE, 2018, pp. 280–285.

[9] H. Lee and H. Kwon, "Contextual deep cnn based hyperspectral classification," in *2016 IEEE International Geoscience and Remote Sensing Symposium (IGARSS)*. IEEE, 2016, pp. 3322–3325.

[10] J.-W. Cho, Y.-C. Seo, S.-H. Jung, S. Kim, and H.-K. Jung, "Fast defect detection of pcb using ultrasound thermography," *The Transactions of the Korean Institute of Electrical Engineers D*, vol. 55, no. 2, pp. 68–71, 2006.

[11] J. Zhang, B. W. Drinkwater, P. D. Wilcox, and A. J. Hunter, "Defect detection using ultrasonic arrays: The multi-mode total focusing method," *NDT & e International*, vol. 43, no. 2, pp. 123–133, 2010.

[12] M. Sharp, R. Ak, and T. Hedberg Jr, "A survey of the advancing use and development of machine learning in smart manufacturing," *Journal of manufacturing systems*, vol. 48, pp. 170–179, 2018.

[13] J. Wang, Y. Ma, L. Zhang, R. X. Gao, and D. Wu, "Deep learning for smart manufacturing: Methods and applications," *Journal of Manufacturing Systems*, vol. 48, pp. 144–156, 2018.

[14] J.-K. Park, B.-K. Kwon, J.-H. Park, and D.-J. Kang, "Machine learning-based imaging system for surface defect inspection," *International Journal of Precision Engineering and Manufacturing-Green Technology*, vol. 3, no. 3, pp. 303–310, 2016.

[15] T. Dutta, J. Sil, and P. Chottopadhyay, "Condition monitoring of electrical equipment using thermal image processing," in *2016 IEEE First International Conference on Control, Measurement and Instrumentation (CMI)*. IEEE, 2016, pp. 311–315.

[16] R. C. Gonzales and R. E. Woods, "Digital image processing," 2002.

[17] R. Kumar and M. Rattan, "Analysis of various quality metrics for medical image processing," *International Journal of Advanced Research in Computer Science and Software Engineering*, vol. 2, no. 11, pp. 137–144, 2012.

[18] D. G. Lowe, "Distinctive image features from scale-invariant keypoints," *International journal of computer vision*, vol. 60, no. 2, pp. 91–110, 2004.

[19] Q. Huynh-Thu and M. Ghanbari, "Scope of validity of psnr in image/video quality assessment," *Electronics letters*, vol. 44, no. 13, pp. 800–801, 2008.

[20] Z. Wang, A. C. Bovik, H. R. Sheikh, and E. P. Simoncelli, "Image quality assessment: from error visibility to structural similarity," *IEEE transactions on image processing*, vol. 13, no. 4, pp. 600–612, 2004.

[21] A. Hore and D. Ziou, "Image quality metrics: Psnr vs. ssim," in *2010 20th international conference on pattern recognition*. IEEE, 2010, pp. 2366–2369.

[22] Y. LeCun, L. Bottou, Y. Bengio, and P. Haffner, "Gradient-based learning applied to document recognition," *Proceedings of the IEEE*, vol. 86, no. 11, pp. 2278–2324, 1998.

[23] A. Krizhevsky, I. Sutskever, and G. E. Hinton, "Imagenet classification with deep convolutional neural networks," *Communications of the ACM*, vol. 60, no. 6, pp. 84–90, 2017.

[24] C. Szegedy, W. Liu, Y. Jia, P. Sermanet, S. Reed, D. Anguelov, D. Erhan, V. Vanhoucke, and A. Rabinovich, "Going deeper with convolutions," in *Proceedings of the IEEE conference on computer vision and pattern recognition*, 2015, pp. 1–9.

[25] K. Simonyan and A. Zisserman, "Very deep convolutional networks for large-scale image recognition," *arXiv preprint arXiv:1409.1556*, 2014.

[26] K. He, X. Zhang, S. Ren, and J. Sun, "Deep residual learning for image recognition," in *Proceedings of the IEEE conference on computer vision and pattern recognition*, 2016, pp. 770–778.

[27] C. Zhang, W. Shi, X. Li, H. Zhang, and H. Liu, "Improved bare pcb defect detection approach based on deep feature learning," *The Journal of Engineering*, vol. 2018, no. 16, pp. 1415–1420, 2018.

[28] A. Ng *et al.*, "Sparse autoencoder," *CS294A Lecture notes*, vol. 72, no. 2011, pp. 1–19, 2011.

[29] S. Khalilian, Y. Hallaj, A. Balouchestani, H. Karshenas, and A. Mohammadi, "Pcb defect detection using denoising convolutional autoencoders," *arXiv preprint arXiv:2008.12589*, 2020.

[30] G. Koch, R. Zemel, and R. Salakhutdinov, "Siamese neural networks for one-shot image recognition," in *ICML deep learning workshop*, vol. 2. Lille, 2015.

[31] M. A. Reza, Z. Chen, and D. J. Crandall, "Deep neural network–based detection and verification of microelectronic images," *Journal of Hardware and Systems Security*, vol. 4, no. 1, pp. 44–54, 2020.

[32] A. Said and V. Torra, *Data Science in Practice*. Springer, 2019.

[33] R. Girshick, J. Donahue, T. Darrell, and J. Malik, "Rich feature hierarchies for accurate object detection and semantic segmentation," in *Proceedings of the IEEE conference on computer vision and pattern recognition*, 2014, pp. 580–587.

[34] G. Ross, "Fast r-cnn," in *Proceedings of the IEEE international conference on computer vision*, 2015, pp. 1440–1448.

[35] S. Ren, K. He, R. Girshick, and J. Sun, "Faster r-cnn: Towards real-time object detection with region proposal networks," in *Advances in neural information processing systems*, 2015, pp. 91–99.

[36] K. He, G. Gkioxari, P. Dollár, and R. Girshick, "Mask r-cnn," in *Proceedings of the IEEE international conference on computer vision*, 2017, pp. 2961–2969.

[37] J. Redmon, S. Divvala, R. Girshick, and A. Farhadi, "You only look once: Unified, real-time object detection," in *Proceedings of the IEEE conference on computer vision and pattern recognition*, 2016, pp. 779–788.

[38] J. R. Uijlings, K. E. Van De Sande, T. Gevers, and A. W. Smeulders, "Selective search for object recognition," *International journal of computer vision*, vol. 104, no. 2, pp. 154–171, 2013.

초록

비접촉식 PCBA 불량 검출을 위한 열화상 이미지의 딥러닝 분석

류시윤
서울대학교 공학전문대학원
응용공학과 응용공학전공

전자 제품의 대량 생산을 위해서 회로 내 검사 방식을 적용하여, 인쇄회로 기판 조합(PCBA) 품질 테스트를 실시한다. 회로 내 검사 방식은 저항값과 전기용량을 측정할 수 있는 장점이 있다. 그러나, 회로 내 검사 방식은 고정대를 사용해야 하기에, 가격적으로 비싸고, 자주 교체해야 하는 단점이 있다. 고정대에 사용되는 바늘은 PCBA 불량 발생의 원인이 되기도 한다.

본 논문에서는 고정대와 회로 내 검사 방식을 적용하지 않고, PCBA의 불량을 검출할 수 있는 비접촉 테스트 방안을 제시한다. 열화상 이미지의 비교 및 딥러닝 분석을 통한 비접촉식 불량 검출 방안이다. 정상품의 열화상 이미지와 불량품의 열화상 이미지를 비교하여, PCBA 접촉없이 불량품을 검출하고, 불량이 있는 구역을 구분한다. 외형적 특성이 존재하지 않는 칩 저항, 칩콘덴서와 같은 부품 검사에 기존 비접촉 비전 검사 방안을 적용할 수 없다. 기존 비접촉 테스트 방안을 검토하고, 제안된 열화상 이미지 분석 방안과 비교해 본다.

열화상 이미지는 규칙 기반 객체 검출 방법(SSIM) 및 딥러닝 분석 방법(CNN, RCNN, AutoEncoder)을 적용하여 검토하였다. 생산성 향상과 스마트 제조 실현을 위해 생산 라인에 적용 가능한 최적의 방법을 제시하고자 합니다.

Keywords : 비접촉 검사, 딥러닝, 불량 검출, 열화상 이미지

Student Number : 2019-27335